frontiers | Frontiers in Immunology

TYPE Original Research
PUBLISHED 08 January 2024
DOI 10.3389/fimmu.2023.1296148

OPEN ACCESS

EDITED BY
William Anderson Paxton,
University of Liverpool, United Kingdom

REVIEWED BY
Helena Nunes-Cabaço,
Universidade de Lisboa, Portugal
Shetty Ravi Dyavar,
Adicet Bio, Inc, United States

*CORRESPONDENCE
Vasilis Kosmoliaptsis
vk256@cam.ac.uk

RECEIVED 18 September 2023
ACCEPTED 06 December 2023
PUBLISHED 08 January 2024

CITATION
Priddey A, Chen-Xu MXH, Cooper DJ, MacMillan S, Meisl G, Xu CK, Hosmillo M, Goodfellow IG, Kollyfas R, Doffinger R, Bradley JR, Mohorianu II, Jones R, Knowles TPJ, Smith R and Kosmoliaptsis V (2024) Microfluidic antibody profiling after repeated SARS-CoV-2 vaccination links antibody affinity and concentration to impaired immunity and variant escape in patients on anti-CD20 therapy. *Front. Immunol.* 14:1296148. doi: 10.3389/fimmu.2023.1296148

Microfluidic antibody profiling after repeated SARS-CoV-2 vaccination links antibody affinity and concentration to impaired immunity and variant escape in patients on anti-CD20 therapy

Ashley Priddey[1], Michael Xin Hua Chen-Xu[2,3], Daniel James Cooper[2,3], Serena MacMillan[1], Georg Meisl[4], Catherine K. Xu[4], Myra Hosmillo[5], Ian G. Goodfellow[5], Rafael Kollyfas[6], Rainer Doffinger[7], John R Bradley[2,3], Irina I Mohorianu[6], Rachel Jones[2,3], Tuomas P. J. Knowles[3,8], Rona Smith[2,3] and Vasilis Kosmoliaptsis[1,9]*

[1]Department of Surgery, University of Cambridge, Addenbrooke's Hospital, Cambridge, United Kingdom, [2]Department of Medicine, University of Cambridge School of Clinical Medicine, Cambridge, United Kingdom, [3]Department of Medicine, Cambridge University Hospitals NHS Foundation Trust, Cambridge, United Kingdom, [4]Centre for Misfolding Diseases, Yusuf Hamied Department of Chemistry, University of Cambridge, Cambridge, United Kingdom, [5]Department of Pathology, Division of Virology, University of Cambridge, Cambridge, United Kingdom, [6]Wellcome-MRC Cambridge Stem Cell Institute, Jeffrey Cheah Biomedical Centre, University of Cambridge, Cambridge, United Kingdom, [7]Department of Clinical Biochemistry and Immunology, Addenbrooke's Hospital, Cambridge, United Kingdom, [8]Cavendish Laboratory, Department of Physics, University of Cambridge, Cambridge, United Kingdom, [9]NIHR Blood and Transplant Research Unit in Organ Donation and Transplantation at the University of Cambridge and the NIHR Cambridge Biomedical Research Centre, Cambridge, United Kingdom

Background: Patients with autoimmune/inflammatory conditions on anti-CD20 therapies, such as rituximab, have suboptimal humoral responses to vaccination and are vulnerable to poorer clinical outcomes following SARS-CoV-2 infection. We aimed to examine how the fundamental parameters of antibody responses, namely, affinity and concentration, shape the quality of humoral immunity after vaccination in these patients.

Methods: We performed in-depth antibody characterisation in sera collected 4 to 6 weeks after each of three vaccine doses to wild-type (WT) SARS-CoV-2 in rituximab-treated primary vasculitis patients (n = 14) using Luminex and pseudovirus neutralisation assays, whereas we used a novel microfluidic-based immunoassay to quantify polyclonal antibody affinity and concentration against both WT and Omicron (B.1.1.529) variants. We performed comparative antibody profiling at equivalent timepoints in healthy individuals after three antigenic exposures to WT SARS-CoV-2 (one infection and two vaccinations; n = 15) and in convalescent patients after WT SARS-CoV-2 infection (n = 30).

10.3389/fimmu.2023.1296148

Results: Rituximab-treated patients had lower antibody levels and neutralisation titres against both WT and Omicron SARS-CoV-2 variants compared to healthy individuals. Neutralisation capacity was weaker against Omicron versus WT both in rituximab-treated patients and in healthy individuals. In the rituximab cohort, this was driven by lower antibody affinity against Omicron versus WT [median (range) K_D: 21.6 (9.7–38.8) nM vs. 4.6 (2.3–44.8) nM, p = 0.0004]. By contrast, healthy individuals with hybrid immunity produced a broader antibody response, a subset of which recognised Omicron with higher affinity than antibodies in rituximab-treated patients [median (range) K_D: 1.05 (0.45–1.84) nM vs. 20.25 (13.2–38.8) nM, p = 0.0002], underpinning the stronger serum neutralisation capacity against Omicron in the former group. Rituximab-treated patients had similar anti-WT antibody levels and neutralisation titres to unvaccinated convalescent individuals, despite two more exposures to SARS-CoV-2 antigen. Temporal profiling of the antibody response showed evidence of affinity maturation in healthy convalescent patients after a single SARS-CoV-2 infection, which was not observed in rituximab-treated patients, despite repeated vaccination.

Discussion: Our results enrich previous observations of impaired humoral immune responses to SARS-CoV-2 in rituximab-treated patients and highlight the significance of quantitative assessment of serum antibody affinity and concentration in monitoring anti-viral immunity, viral escape, and the evolution of the humoral response.

KEYWORDS

antibody affinity, rituximab, SARS-CoV-2 vaccination, neutralisation capacity, Omicron (B.1.1.529), antibody concentration, immunocompromised, SARS-CoV-2 infection

Introduction

SARS-CoV-2 infection (COVID-19) is of ongoing clinical concern for patients with primary systemic vasculitis, particularly those receiving repeated dosing with B cell-depleting therapies, such as the anti-CD20 agent, rituximab. Patients with autoimmune/inflammatory conditions on immunosuppressive therapy, particularly those on anti-CD20 therapies (1, 2), are vulnerable to poorer clinical outcomes following SARS-CoV-2 infection, including hospitalisation and death (3, 4). Given this and the suboptimal humoral immune responses after SARS-CoV-2 vaccination observed in those receiving anti-CD20 therapies (5–7), subsequent SARS-CoV-2 vaccine doses, i.e., "boosters", have been recommended for these patient groups in several jurisdictions (8–10), including those with primary systemic vasculitis (11).

Humoral immune responses after primary vaccination using vaccines targeted against the original (ancestral, wild-type) strain of SARS-CoV-2, e.g., the mRNA vaccines Pfizer BioNTech BNT162b2 (Pfizer) and mRNA-1273 (Moderna) or the adenovirus-vector based vaccines Oxford-AstraZeneca ChAdOx1 nCoV-19 (AZ) or Ad26.COV2-S (Johnson & Johnson), are often suboptimal among patients receiving anti-CD20 therapies. Specifically, titres of antibodies directed against the spike protein subunit (anti-spike IgG) and/or receptor binding domain (anti-RBD IgG) of SARS-CoV-2 and the proportion of patients on anti-CD20 therapy who seroconvert following primary vaccination are lower compared to those not on such therapy and healthy controls (5, 6, 12, 13). Furthermore, of patients on anti-CD20 therapies who seroconvert after primary vaccination, many have lower neutralisation titres compared to those on other immunosuppressants and healthy controls (14–16). Although neutralising antibody titres and, to a lesser extent, anti-spike IgG and anti-RBD IgG titres, derived from primary vaccination with vaccines targeting the original strain of SARS-CoV-2, correlate with protection against symptomatic infection from the ancestral virus (17), significant reductions in the neutralisation capacity of these antibodies have been observed against subsequent SARS-CoV-2 variants of concern, such as the B.1.617.2 variant (Delta) (17) and the B.1.1.529 variant and its sublineages (Omicron) (18–20), which harbour mutations in the spike protein that modify the critical domain for virus-neutralising antibodies (21,

22). SARS-CoV-2-specific T-cell responses following vaccination, which may be protective against severe infection (23, 24), appear largely preserved among anti-CD20-treated patients (5), although the clinical significance of these responses in such patients remains unclear. Consequently, primary systemic vasculitis patients receiving anti-CD20 therapies may still be vulnerable to severe SARS-CoV-2 infection even if they develop antibodies following primary vaccination, particularly given the emergence of variants with humoral immune escape properties.

We have recently developed a novel immunoassay, microfluidic antibody affinity profiling (MAAP), for in-solution quantification of the fundamental parameters of the antibody response, namely, affinity and concentration, directly in serum (25), and used it to characterise antibody profiles against wild-type (WT) SARS-CoV-2 in convalescent sera (26) and to study the role of cross-reactivity as a consequence of memory reactivation after acute SARS-CoV-2 infection (27). MAAP can distinguish samples containing low levels of high-affinity antibodies from samples with high levels of low-affinity antibodies, which would otherwise exhibit the same EC_{50} (half-maximal effective concentration) using an ELISA-based technique (26, 27). Thus, MAAP may allow for a more granular assessment of antibody responses following antigen exposure and provide insights into the potency of the humoral response against emerging variants of concern. Nevertheless, a recent study exploring antibody profiles in pre-Omicron sera from largely immunocompetent patients with a variety of antigenic exposures to SARS-CoV-2 antigens (including after one or more doses of WT vaccine or after infection or both) showed similar antibody affinities against Omicron versus WT or Delta spike antigens, albeit the timing of serum sampling for antibody assessment in this study was widely variable (28).

Several recently published studies have assessed humoral responses following booster vaccination(s) among cohorts of patients with autoimmune/inflammatory conditions on anti-CD20 therapies, which have included vasculitis patients (29–34), although few have examined primary systemic vasculitis patients specifically (35–37). The primary aim of this study was to perform in-depth serological characterisation of antibody responses at pre-specified timepoints after repeated vaccination (specifically after the second and third doses) against SARS-CoV-2 in pre-Omicron sera from rituximab-treated patients with primary systemic vasculitis. Along with serological profiling using solid-phase and neutralisation assays, we capitalised on our recently described microfluidic-based immunoassay to quantify antibody affinity and concentration against WT versus Omicron strains of SARS-CoV-2. We subsequently performed antibody profiling at equivalent timepoints in a cohort of healthy individuals after similar, repeated antigenic exposure to SARS-CoV-2. Finally, we compared the serological response to repeated vaccination in rituximab-treated patients to that in unvaccinated, convalescent patients after a single exposure to WT SARS-CoV-2 infection. We found suboptimal humoral immunity even after repeated vaccination in rituximab-treated patients and highlighted the role of quantitative assessment of serum antibody affinity and concentration in monitoring anti-viral immunity, viral escape, and the evolution of the humoral response.

Methods

Cohort description

Patients with primary systemic vasculitides were recruited from a prospective observational cohort study investigating SARS-CoV-2 vaccine responses among renal populations at the Department of Nephrology at Cambridge University Hospitals NHS Foundation Trust (CUH) (ethics reference: 20/EM/0180), as previously described (38). Patients receiving intravenous immunoglobulin (IVIg) or plasma exchange were excluded as potential confounders of vaccine responses. Samples from the healthcare worker cohort were part of the asymptomatic staff screening programme at CUH, as previously described (39). All staff members were invited to participate in the serological screening programme and provided written informed consent (NIHR BioResource—COVID-19 Research cohort; ethics reference: 17/EE/0025, IRAS ID: 220277). The study participants in the convalescent patient cohort were recruited between March 2020 and July 2020 from patients attending CUH with nucleic acid confirmed diagnosis of COVID-19 (ethics reference: 17/EE/0025), as previously described (40). All participants provided informed consent.

Blood samples were taken at approximately 4 to 6 weeks after each sensitisation/vaccination event (1A, 2A, or 3A) with the flexibility to align with routine clinical tests and access to blood testing facilities wherever possible. Blood samples for the convalescent cohort were taken at the timepoints specified (1A = 1 month and 1B = 3 months from diagnosis of COVID-19). Clinical data collected from electronic medical records and patient interviews included baseline demographics, changes to immunosuppressive medication over time, and data on episodes of SARS-CoV-2 infection.

Fluorescent labelling of proteins

Recombinant SARS-CoV-2 spike RBD proteins from WT (#40592-V08H) and Omicron (B.1.1.529; #40592-V08H121) strains were purchased from Sino Biological (Beijing, China) and labelled with AlexaFluor 647 as previously described (25). In brief, 100 µg of SARS-CoV-2 RBD protein was resuspended in H_2O and mixed with $NaHCO_3$ (pH 8.3) buffer to a final concentration of 100 mM. Dimethyl sulfoxide (DMSO)-reconstituted AlexaFluor™ 647 *N*-hydroxysuccinimidyl ester (Thermo Fisher Scientific, Waltham, MA, USA) was added at a threefold molar excess, and the reaction was incubated at room temperature for 1 h. The reaction mixture underwent size-exclusion chromatography in phosphate-buffered saline (PBS), pH 7.4, using an ÄKTA pure system and a Superdex 200 Increase 10/300 column (Cytiva, Marlborough, MA, USA) to separate the labelled protein from the free fluorophore. Labelled protein fractions were pooled and concentrated using an Amicon Ultra-0.5 10K centrifugal filter device (Millipore, Billerica, MA, USA) and glycerol was added to a concentration of 10% (w/v) prior to snap freezing in LN_2 and storage at −80°C. Upon thawing and before use, protein concentrations were quantified via Nanodrop using the molar extinction coefficient.

Antibody affinity and concentration measurements

The affinity and concentration of anti-RBD antibodies within patient sera were determined using MAAP (26). The hydrodynamic radius (R_H) of 1–500 nM AlexaFluor™ 647-labelled spike RBD proteins were measured in the presence of MAAP buffer (PBS containing 5% human serum albumin (Sigma, St. Louis, MO, USA), 10% (w/v) glycerol, and 0.05% Tween-20) and varying concentrations (0%–50%) of patient serum via microfluidic diffusional sizing (MDS) using the Fluidity One-W or One-M instruments (Fluidic Analytics Ltd., Cambridge, UK) after a 1-h incubation on ice. The background fluorescence within each diffused and non-diffused microfluidic stream was subtracted from the MDS data for the specific serum concentrations, and Bayesian inference analysis was used to constrain the values of affinity (K_D) and antibody binding sites ([Ab]), as previously described (25, 26). Serum samples that enabled constrained K_D and [Ab] values to be measured (with both upper and lower 95% confidence intervals) were considered quantifiable. Those that had an [Ab]/K_D ratio of >2 were labelled as fully quantifiable (Q), and those that had a [Ab]/K_D of 1–2 were considered to be at the border of sensitivity for full quantification (B; borderline). Samples that yielded no measured increase in the RBD hydrodynamic radius after serum incubation (N; non-binders) and/or those samples that yielded incomplete K_D and/or [Ab] bounds (U; unquantifiable due to inability to fully constrain 95% confidence interval lower bounds for both parameters) were deemed non-quantifiable and excluded from subsequent analysis.

Luminex assay

Serum antibody reactivity to SARS-CoV-2 WT spike, RBD, and nucleocapsid proteins was assessed using a United Kingdom Accreditation Service (UKAS)-accredited Luminex platform, as previously reported (41). In brief, patient serum diluted 1/100 was incubated for 1 h at room temperature with WT spike, RBD, or nucleocapsid proteins covalently coupled to distinct carboxylated beads in a triplex assay. The liquid phase was aspirated, and beads were washed with 10 mM PBS/0.05% Tween-20 three times before incubation with phycoerythrin (PE)-conjugated anti-human IgG-Fc antibody (Leinco, Fenton, MO, USA/Biotrend, Palo Alto, CA, USA) for 30 min. Beads were washed again as above and resuspended in 100 µl PBS/Tween before being analysed on a Luminex analyser (Luminex, Austin, TX, USA/R&D Systems, Minneapolis, MN, USA) using Exponent Software V31. Specific binding of antibodies to each protein was reported as the mean fluorescence intensity (MFI).

Pseudotype neutralisation assay

Sera were heat-inactivated at 56°C for 30 min and then frozen in aliquots at −80°C. Virus neutralisation assays were performed on HEK293T cells that were transiently transfected with ACE2 using a SARS-CoV-2 spike pseudotyped virus expressing luciferase, as previously described (42). Pseudotyped virus was prepared by transfection of HEK293T cells using the Fugene HD transfection system (Promega, Madison, WI, USA), as previously described (42). Pseudotyped virus was incubated with serial dilution of heat-inactivated human serum samples in duplicate for 1 h at 37°C. Virus-only and cell-only controls were included. Freshly trypsinised HEK293T ACE2-expressing cells were added to each well. Following 48-h incubation in a 5% CO_2 environment at 37°C, luminescence was measured using the Bright-Glo Luciferase assay system (Promega), and neutralisation was calculated relative to virus-only controls. Neutralising antibody titres at 50% inhibition (ND_{50}) were calculated in GraphPad Prism.

Statistical analysis

Statistical analyses were carried out using GraphPad Prism v9.5.0 and in *R* version 4.2.3. Comparison of paired datasets was performed using the Wilcoxon matched paired signed-rank test to track the trending pattern between the paired samples, and the Mann–Whitney U test was used to compare distributions between two groups. Multiple group differences were analysed using the Kruskal–Wallis tests, and pairwise differences across groups were examined using Dunn's test, with the Benjamini–Hochberg corrections to account for potential false discovery from multiple comparisons. Linear regression models were optimised to assess relationships between variables, where indicated. All p-values are two-tailed where ns > 0.05, * ≤ 0.05, ** ≤ 0.01, *** ≤ 0.001, and **** ≤ 0.0001.

For visualisation, scatter, violin, and boxplots were generated using the ggplot2 package (version 3.4.2). Contour lines were superimposed upon a scatter plot using the geom_hdr function provided by the ggdensity package (version 1.0.0). Correlation values, including both Pearson's and Spearman's coefficients, were determined using the cor.test function of the stats package. These values were then annotated on the plots using the annotate function inherent to ggplot2. The summary heatmap was created using the ComplexHeatmap package (version 2.15.4).

Results

Anti SARS-CoV-2 antibody profiling in rituximab-treated vasculitis patients

We identified a cohort of 14 patients with primary systemic vasculitis treated with rituximab (RTX cohort) who had been recruited in a prospective observational cohort study investigating SARS-CoV-2 vaccine responses among renal populations (38) and had paired samples, collected at pre-specified timepoints, after the first, second, and third vaccine doses. The patient demographics are

10.3389/fimmu.2023.1296148

summarised in Supplementary Table 1. The majority of patients (79%) had rituximab within 12 months prior to the first vaccine dose, and 64% had additional rituximab between vaccine doses. Serological responses to wild-type SARS-CoV-2 spike and RBD, as assessed using an accredited Luminex immunoassay 4–6 weeks after each vaccine dose, are shown in Figure 1. Overall, 57% of the cohort showed a positive anti-spike response [median (range) MFI: 3,958 (59–22,509)] and 14% a positive anti-RBD response [median (range) MFI: 115 (46–2,437)] after the first vaccine dose. Seroconversion and Luminex MFI values increased significantly after the second vaccine dose, both against spike [100% positive; median (range) MFI: 27,713 (9,047–32,716); $p < 0.0001$, Mann–Whitney test] and RBD [71% positive; median (range) MFI: 5,301 (33–31,509); $p = 0.0384$, Mann–Whitney test], and remained stable after the third vaccine dose [100% anti-spike positive; median (range) MFI: 27,356 (2,398–32,662); $p = 0.5007$; and 64% anti-RBD positive; median (range) MFI: 19,741 (127–32,331); $p = 0.2915$ between second and third vaccine doses; Mann–Whitney test]. Notably, four patients showed consistently negative anti-RBD responses, and 42% of sera with significant anti-spike antibody reactivity (n = 33) were negative against SARS-CoV-2 RBD (n = 14). Patients who received additional rituximab between the second and third vaccine doses (n = 6) did not have significantly different antibody responses compared to those who did not [median (range) MFI after the third vaccine: anti-spike; 32,552 (9,047–32,716) versus 27,356 (13,984–32,662), $p = 0.5368$, anti-RBD; 19,176 (33–31,501.8) versus 26,931 (136–32,331), $p = 0.4286$, Mann–Whitney tests].

Neutralising antibodies against WT were detectable in 50% of patients after both the second and third vaccine doses with overall similar 50% neutralising dose titres (ND_{50}) between the two timepoints [median (range) ND_{50} of 207 (20–2,254) versus 240 (20–7,468), $p = 0.5890$, Mann–Whitney test]. Nevertheless, individual patient responses after vaccination were variable with neutralising titres increasing in six patients and decreasing in three patients, whereas a further five patients did not develop neutralising antibodies after three vaccine doses (Figure 2A). To provide a more in-depth analysis of serological responses in these patients, we further characterised anti-RBD antibodies by MAAP. Consistent with Luminex, MAAP showed that the affinity (K_D) and concentration [(Ab)] of antibodies against WT RBD did not change significantly between the second and third vaccine doses (Figures 2B, C). All neutralising sera were quantifiable by MAAP, whereas non-neutralising sera could not be quantified due to either undetectable/low anti-RBD antibody levels (n = 10, RBD MFI 33–3,440) or the inability to effectively constrain MAAP parameters (n = 3, RBD MFI 5,301–19,741; Supplementary Figure 1 and Supplementary Table 2; one non-neutralising serum had a missing MFI and showed minimal binding on MAAP). Overall, the affinity of quantifiable anti-WT RBD antibodies ranged widely from 2.3 nM to 44.8 nM, and in patients with increasing neutralisation titres after the third vaccine dose, this was driven predominantly by an increase in antibody concentration rather than improvement in affinity.

Analysis of serum antibody reactivity against the Omicron variant showed that only 3/14 (21%) and 4/14 (29%) patients developed neutralising antibodies after the second and third vaccine doses, respectively. Similar to WT, individual patient responses varied, although more patients had measurable Omicron anti-RBD antibodies after the third vaccine dose (seven patients had an improved response and three patients had a worse response to Omicron RBD), as determined by MAAP (Figures 2D–F and Supplementary Table 2). Overall, the affinity of anti-Omicron RBD antibodies varied from 9.7 to 38.8 nM, and their concentration varied from 56.5 to 1,080 nM, with no significant difference in either parameter between the two timepoints. Importantly, there was decreased neutralisation capacity against Omicron compared to

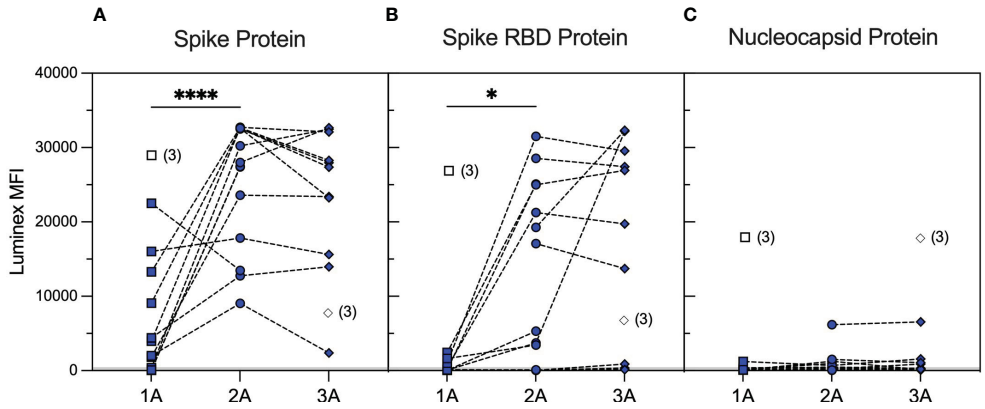

FIGURE 1
Serological responses to wild-type SARS-CoV-2 antigens in rituximab-treated patients after repeated vaccination. SARS-CoV-2 antibody profiles as determined using Luminex. The y-axis depicts mean fluorescence intensity (MFI) levels. Sera were assessed at approximately 1 month after the first (1A, squares), second (2A, circles), and third (3A, diamonds) vaccine doses against spike **(A)**, RBD **(B)**, and nucleocapsid **(C)** antigens. Symbols represent the MFI values for one sample, whereas dotted lines connect samples from the same patient taken at different timepoints. Unfilled symbols represent samples (number) where Luminex MFI data were unavailable. Luminex MFI values increased significantly after the second vaccine dose, against both spike (2A vs. 1A timepoints; $p < 0.0001$, Mann–Whitney test) and RBD (2A vs. 1A timepoints; $p = 0.0384$, Mann–Whitney test), and remained stable after the third vaccine dose (3A vs. 2A; $p = 0.5007$ for anti-spike and $p = 0.2915$ for anti-RBD MFI, Mann–Whitney test). ****: <0.0001; *: <0.05.

10.3389/fimmu.2023.1296148

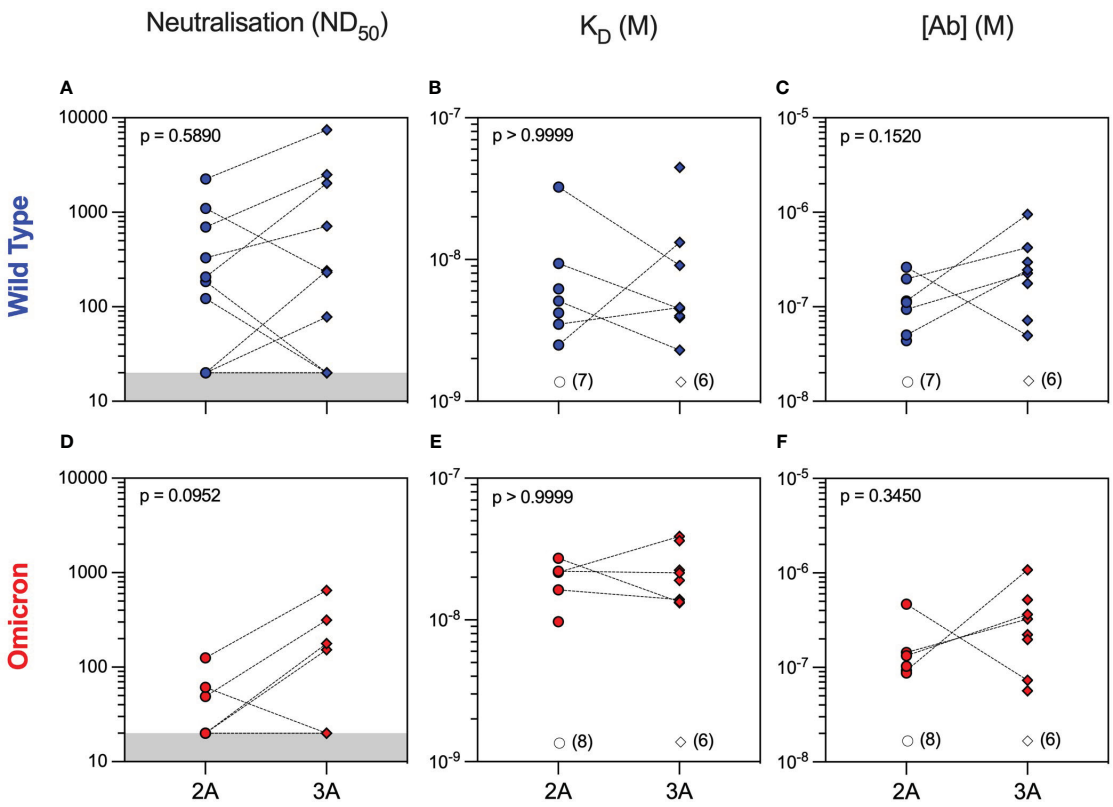

FIGURE 2
Serum neutralisation capacity and microfluidic antibody affinity profiling against wild-type and Omicron variants in rituximab-treated patient cohort. Sera from rituximab-treated vasculitis patients were assessed at 1 month after the second (2A, circles, n = 14) and third (3A, diamonds, n = 14) vaccine doses for their neutralising capacity (ND_{50}: 50% neutralising dose titre) against both wild-type **(A)** and Omicron **(D)** variants. All sera were quantified using microfluidic antibody affinity profiling (MAAP) to measure the affinity (K_D, M) and concentration ([Ab], M) of antibody binding sites that specifically bind either the wild-type **(B, C)** or Omicron **(E, F)** SARS-CoV-2 spike RBD domains. There were no significant differences between timepoints for any of the comparisons using either paired (Wilcoxon paired signed-rank test) or unpaired (Mann–Whitney) statistical assessments (p-values from Mann–Whitney tests are shown). Dotted lines connect samples taken from the same patient at different timepoints. Grey regions represent the lower limit of the neutralisation assay. Unfilled symbols represent the samples (number) where MAAP data were unobtainable due to non-binding or unquantifiable binding.

WT after both the second and third vaccine doses (Figures 3A–C). MAAP analysis showed that this difference was driven by significantly weaker antibody affinity to the Omicron versus WT RBD [median (range) K_D: 21.6 (9.7–38.8) nM vs. 4.6 (2.3–44.8) nM, respectively, p = 0.0004, Wilcoxon paired ranked test] rather than by differences in antibody concentration [median (range) (Ab): 171 (56.5–1,080) nM vs. 177 (43.7–952) nM, respectively, p = 0.2412, Wilcoxon paired ranked test], and this was consistent at both timepoints (Figures 3D, E and Supplementary Figure 2). Overall, 14 (50%) samples had no neutralisation against either variant, whereas five patients did not develop neutralising antibodies at either timepoint. Taken together, the above results demonstrate that rituximab-treated patients developed widely variable antibody responses to SARS-CoV-2 after repeated vaccination, which, when quantifiable by MAAP, varied by 20-fold in affinity. Overall, neutralising antibody responses were often absent even after three vaccine doses; when present, neutralisation capacity was significantly weaker against Omicron versus WT SARS-CoV-2 strains, and this difference was driven by the weaker affinity of vaccine-induced antibodies against the Omicron strain.

Anti-SARS-CoV-2 antibody profiling in healthy individuals versus rituximab-treated patients

We next hypothesised that the quality of the antibody response would vary significantly in healthy individuals compared to rituximab-treated patients following antigenic exposure to SARS-CoV-2. To investigate this, we profiled antibody responses in healthcare workers (HCWs) recruited at Cambridge University Hospital who, similar to the vasculitis cohort, had three exposures to SARS-CoV-2 antigen, consisting of an asymptomatic infection to SARS-CoV-2 prior to the emergence of the Omicron variant and two subsequent vaccine doses (see Methods and Supplementary Table 1). We performed antibody profiling at 4 weeks after the third exposure (second vaccine dose). Luminex analyses showed significantly higher antibody reactivity to WT spike and RBD in HCWs versus rituximab-treated patients (Supplementary Figure 3; Supplementary Table 4). Similar to rituximab-treated patients, neutralisation titres in HCWs were significantly higher against the WT versus the Omicron variant. Further profiling by MAAP suggested this difference was

10.3389/fimmu.2023.1296148

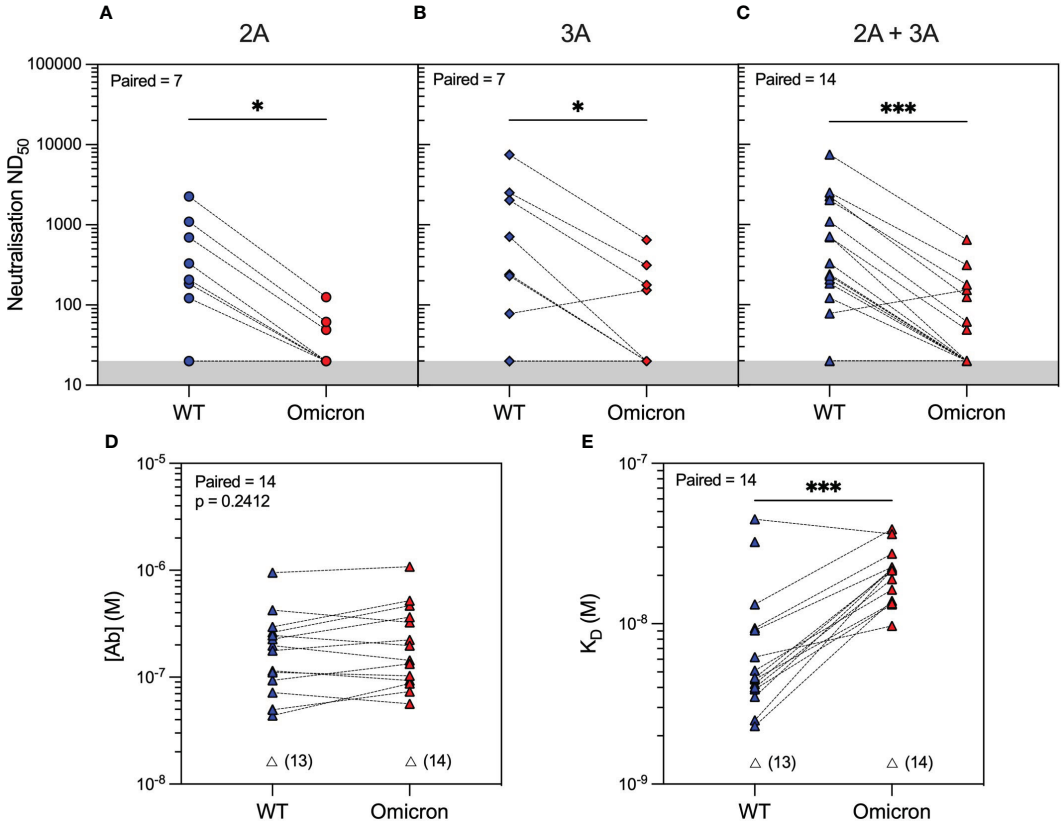

FIGURE 3
SARS-CoV-2 antibody profiling in rituximab-treated patients showed reduced neutralising capacity against the Omicron compared to wild-type (WT) variants driven by weaker antibody affinity to the Omicron spike RBD. Neutralising capacity (ND_{50}) of serum from rituximab-treated vasculitis patients against the Omicron variant (red symbols) compared to the WT variant (blue symbols) at 1 month after the second vaccine dose (**A**; 2A, circles, p = 0.0156), third vaccine dose (**B**; 3A, diamonds, p = 0.0312), or when data from both timepoints were combined (**C**; 2A+3A, triangles, p = 0.0002). Microfluidic antibody affinity profiling to measure antibody affinity (K_D, M) and binding site concentration ([Ab], M) demonstrated no difference in the concentration of antibodies recognising the WT and Omicron RBD variants (**D**, p = 0.2412) but weaker antibody affinity against the Omicron strain (**E**, p = 0.0004). Dotted lines connect identical samples assessed against different variants. Unfilled symbols represent the samples (number) where MAAP data were unobtainable due to insufficient or unquantifiable binding. p-Values presented are two-tailed from the Wilcoxon paired signed-rank test.

driven by the fact only a fraction of high-affinity serum antibodies recognised the Omicron RBD (Supplementary Figure 3). Compared to rituximab-treated patients (Figure 4), MAAP quantifiable antibodies to WT SARS-CoV-2 in the HCW cohort were of higher concentration [median (range) (Ab) of 236.5 (49.5–952) nM *vs.* 646 (233–2,110) nM, respectively, p = 0.0018, Mann–Whitney test] but of similar affinity [median (range) K_D of 4.6 (2.3–44.8) nM vs. 4.7 (1.2–19.0) nM, respectively, p = 0.5825, Mann–Whitney test], underpinning the higher neutralisation titres in the HCW cohort [median (range) ND_{50} of 49 (20–7,468)] versus 2,522 [864–7,297], p = 0.0004, Mann–Whitney test; Figure 4). Neutralisation titres against the Omicron strain were also higher in HCWs versus rituximab-treated patients [median (range) ND_{50} of 221.5 (24.63–1,225) versus 20 (20–648.7), respectively, p = 0.003, Mann–Whitney test; Figure 4], but this was driven by higher affinity anti-Omicron RBD antibodies in the HCW cohort [median (range) K_D: 1.05 (0.45–1.84) nM vs. 20.25 (13.2–38.8) nM, p = 0.0002, Mann–Whitney test]. Taken together, our results confirm the previously reported impaired antibody responses to SARS-CoV-2 variants of concern in rituximab-treated, immunosuppressed patients compared to healthy individuals and, through MAAP analysis, highlight the significance of the fundamental parameters of the antibody response, namely, antibody affinity and concentration, to anti-viral immunity and virus escape.

Evolution of antibody response to SARS-CoV-2 after infection and vaccination

In the microfluidic-based antibody profiling of the rituximab patient cohort described above, we could not detect evidence of affinity maturation in peripheral blood samples collected after the second compared to the third vaccine doses, despite a median of 185 days (range 141–224 days) between the two timepoints. To investigate whether this observation was specific to the rituximab-treated patients, we next examined the quality of the humoral response after WT SARS-CoV-2 infection in patients during the first wave of the COVID-19 pandemic using samples collected at 1 and 3 months post-infection (see Methods). The demographic characteristics of this cohort (n = 30) are shown in Supplementary Table 1. As shown in Figure 5, we observed wide variation in affinity (K_D range 2.07–34.0 nM) and concentration

10.3389/fimmu.2023.1296148

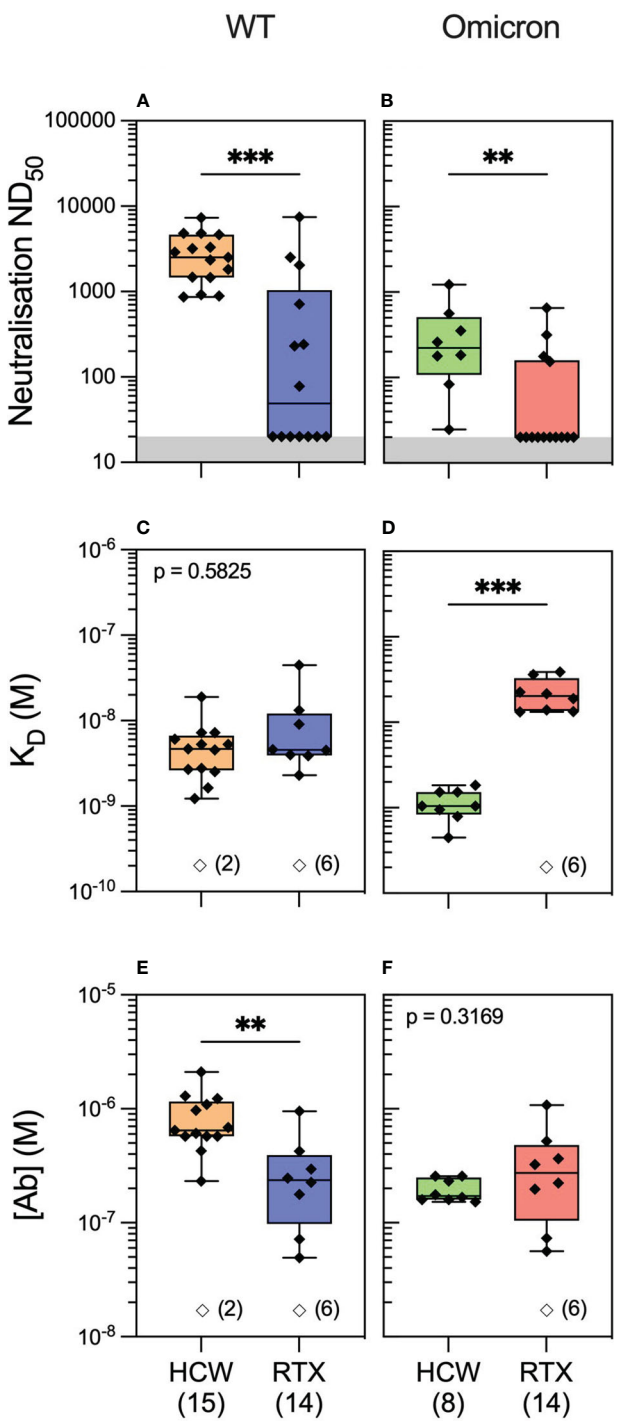

FIGURE 4
Anti-SARS-CoV-2 antibody profiling in healthy individuals versus rituximab-treated patients. Serum neutralising titres (ND_{50}) in healthcare workers (HCWs) versus rituximab (RTX)-treated vasculitis patients 1 month after the third exposure to SARS-CoV-2 antigen (3A) assessed against wild-type (**A**; p = 0.0004) and Omicron strains (**B**; p = 0.003). Comparison of quantifiable antibodies to wild-type SARS-CoV-2 using microfluidic antibody affinity profiling (MAAP) showed similar affinity (**C**; p = 0.5825) but lower abundance in rituximab-treated patients (**E**; p = 0.0018). In contrast, the abundance of antibodies against the RBD Omicron variant was comparable between the cohorts (**F**; p = 0.3169); however, these antibodies were of higher affinity in the HCW cohort (**D**; p = 0.0002). In panels **(A, B)**, the grey region represents the lower limit of detection for the neutralisation assay. Box plots represent the median, range, and interquartile range for each dataset. Unfilled symbols in panels **(C–F)** represent samples (number) where MAAP data were unobtainable due to insufficient or unquantifiable binding. Statistical analysis was carried out for each plot using the Mann–Whitney test, and the presented p-values are two-tailed. **: <0.01; ***: <0.001.

10.3389/fimmu.2023.1296148

(range 7.1–1,120 nM) of the antibody responses to WT RBD at both timepoints. As expected, there was a significant decrease in antibody concentration over time [median (range): 55.6 (7.1–269) nM at 3 months vs. 169 (13–1,120) nM at 1 month post-infection, p = 0.0034, Wilcoxon paired ranked test] and an associated decrease in neutralisation capacity [median (range) ND_{50} of 131 (20–7,983) versus 280 (20–14,580), respectively, p = 0.0296, Wilcoxon paired ranked test]. Nevertheless, we were able to detect evidence of affinity maturation over the same time period, as demonstrated by a decrease in anti-RBD dissociation constant in the majority of patients [median (range) K_D: 6.6 (2.1–14.6) nM at 3 months *vs.* 9.4 (2.1–34) nM at 1 month post-infection, p = 0.0244, Wilcoxon paired ranked test]. Luminex analysis of antibody reactivity to WT spike and RBD showed significantly higher responses at 1 month after infection in the convalescent cohort compared to 1 month after the first vaccine dose in the rituximab cohort; these antibodies in rituximab-treated patients reached similar levels to those in the convalescent cohort after the second and third vaccine doses (Supplementary Figures 4D, E). Comparison of the convalescent cohort at 1 month post-infection with the rituximab-treated patient cohort at equivalent timepoints after the second and third vaccine doses showed similar neutralisation titres against WT SARS-CoV-2 despite exposure to only a single sensitisation event (Figure 6). Corroborating these findings, quantification of WT anti-RBD responses by MAAP showed similar antibody affinity and concentration after the second and third vaccine doses in rituximab-treated patients compared to those in post-infection convalescent patients (Figures 6B, C).

Multidimensional assessment of antibody fingerprints (concentration and affinity) with clinical parameters at the individual patient level

To provide a global perspective of antibody affinity/concentration profiles against WT and Omicron variants, we created integrated 2D density contour plots incorporating MAAP data obtained from the above three patient groups (rituximab-treated vasculitis patients ~1 month after the third vaccine dose *vs.* healthcare workers ~1 month after the third sensitisation event *vs.* COVID-19 convalescent patients ~1 month post-infection). As shown in Figure 7, HCWs clustered separately [high affinity and high (Ab) profiles], whereas the density representations for rituximab-treated and convalescent patients were wider and largely overlapping. As discussed above, a left shift of antibody profiles to the Omicron variant was apparent in rituximab patients with significantly lower affinity compared to anti-Omicron profiles in the HCW cohort. The relationship of antibody fingerprints with clinically relevant parameters showed that the $K_D \times$ [Ab] product was similar between female and male patients, whereas a weak negative correlation was noted with increasing age for anti-WT antibody profiles (Spearman's correlation coefficient $\rho = -0.67$, p = 0.0012; Figures 7B, C). For convalescent patients, the $K_D \times$ [Ab] product tended to be higher in patients with more severe disease (Figure 7D).

We next incorporated serological parameters (MAAP affinity/concentration, Luminex MFI, and ND_{50}) with relevant immunological and demographic variables (SARS-CoV-2 variant, vaccine dose, patient cohort, age, sex, and ethnic background) to provide a comprehensive multidimensional assessment of the single-individual level (Figure 8A), which highlighted the strength of the anti-SARS-CoV-2 response (higher ND_{50}, [Ab], Luminex anti-spike, and anti-RBD MFI) in healthy individuals, compared to rituximab-treated and convalescent patients. We also related antibody WT SARS-CoV-2 serological read-outs obtained from neutralisation, MAAP, and Luminex assays, which showed a strong correlation between ND_{50} and antibody concentration or ND_{50} and Luminex RBD MFI (Spearman's correlation coefficient $\rho = 0.74$, $p = 8.1 \times 10^{-12}$, and $\rho = 0.81$, $p = 5.5 \times 10^{-24}$, respectively; Figures 8B, C) but no relationship between ND_{50} and Luminex RBD MFI with antibody affinity (Supplementary Figure 5). These observations suggest that neutralisation and solid-phase Luminex assays primarily reflect antibody concentrations (Supplementary

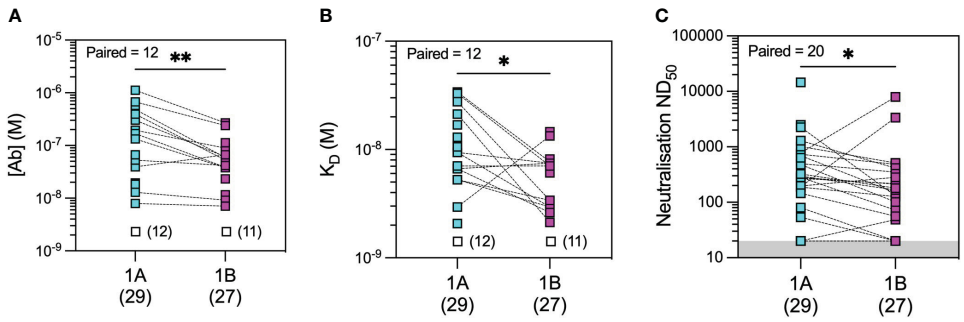

FIGURE 5
Microfluidic antibody affinity profiling (MAAP) of the evolution of the antibody response after infection with wild-type SARS-CoV-2. Anti-SARS-CoV-2 wild-type spike RBD antibody affinity (K_D, M) and binding site concentration ([Ab], M) in sera from convalescent patients at 1 month (1A) and 3 months (1B) post-infection were assessed using MAAP. Panel **(A)** shows that the concentration of antibodies decreased over time (**A**; p = 0.0034), but their affinity against RBD increased (**B**; p = 0.0244), resulting in an overall decrease in serum neutralisation capacity (**C**; p = 0.0296). Dotted lines connect samples taken from the same patient at the two timepoints. Unfilled symbols in panels **(A, B)** represent samples (number) where MAAP data were unobtainable due to insufficient or unquantifiable binding. Presented p-values are two-tailed from the Wilcoxon paired signed-rank test. *: <0.05; **: <0.01.

10.3389/fimmu.2023.1296148

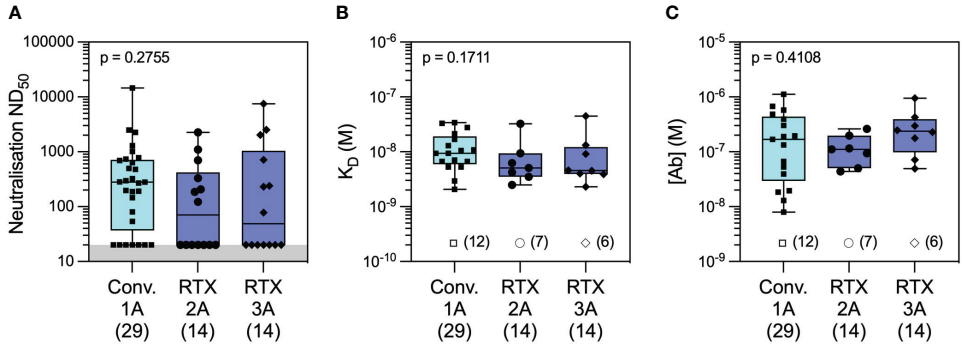

FIGURE 6
Antibody profiling against wild-type SARS-CoV-2 in convalescent versus rituximab-treated patients. Comparison of serum neutralising titres (ND_{50}) in convalescent patients 1 month after wild-type SARS-CoV-2 infection (Conv. 1A) versus in rituximab-treated patients at 1 month following the second (RTX 2A) and third vaccine doses (RTX 3A) showed numerically higher but not statistically different titres in the two cohorts (**A**; Conv. 1A *vs.* RTX 2A: p = 0.2832 and Conv. 1A *vs.* RTX 3A: p = 0.5515). Comparison of quantifiable antibodies to wild-type SARS-CoV-2 using microfluidic antibody affinity profiling (MAAP) showed similar antibody affinity (**B**; Conv. 1A *vs.* RTX 2A: p = 0.2236 and Conv. 1A *vs.* RTX 3A: p = 0.3002) and antibody concentration (**C**; Conv. 1A *vs.* RTX 2A: p > 0.9999 and Conv. 1A *vs.* RTX 3A: p = 0.6399). Box plots represent the median, range, and interquartile range for each dataset. Grey shading in panel A represents the lower assay limit. Unfilled symbols in panels **(B, C)** represent samples (number) where MAAP data were unobtainable due to insufficient or unquantifiable binding. Statistical analysis was carried out using the Kruskal–Wallis ANOVA test (presented) and Dunn's multiple comparisons, and all p-values are two-tailed.

Figure 5C) rather than affinities for MAAP quantifiable samples analysed here.

Discussion

In this study, primary systemic vasculitis patients treated with rituximab had significantly impaired humoral immune responses compared to healthy individuals after three exposures to SARS-CoV-2 antigens, demonstrated by lower anti-spike and anti-RBD antibody levels and lower neutralisation titres against both wild-type and Omicron variants. Despite an incremental increase in antibody levels after the second vaccine dose, no further enhancement of the response was noted after the third dose. Correspondingly, after the third vaccine dose, approximately half and two-thirds of rituximab patients had no detectable neutralising antibodies against WT and Omicron, respectively. Relative to unvaccinated convalescent individuals, rituximab-treated patients had similar anti-spike and anti-RBD antibody levels and similar (albeit numerically lower) neutralisation titres to WT SARS-CoV-2, despite two more exposures to SARS-CoV-2 antigen. Antibodies produced by rituximab-treated patients varied by 20-fold in magnitude in affinity, and the difference in neutralisation capacity between Omicron and WT SARS-CoV-2 was driven by the weaker affinity of vaccine-induced antibodies against the Omicron variant. By contrast, healthy individuals with hybrid immunity in the form of previous infection and two vaccinations produced a broader, high-concentration antibody response as profiled using MAAP, a subset of which recognised Omicron RBD with higher affinity than antibodies in rituximab-treated patients, likely underpinning the more effective neutralisation capacity against Omicron in this group compared to rituximab-treated patients. Finally, we demonstrate that MAAP can assess the evolution of humoral immune responses by direct measurement of polyclonal antibody affinity in serum, without the need for antigen-specific B-cell isolation and antibody sequencing or measurement of antibody dissociation kinetics in solid-phase assays that can be perturbed by avidity-driven interactions (43–45). Accordingly, we detected evidence of affinity maturation within 3 months from primary infection in convalescent patient sera despite a relative decrease in anti-RBD antibody concentration. This was not evident in rituximab-treated patients, even after the third vaccine dose.

Our findings of impaired humoral immune responses after the third SARS-CoV-2 vaccine dose in our primary systemic vasculitis patient cohort receiving anti-CD20 therapies are in agreement with the recently published literature, although we are unaware of any other groups who have quantified these using a combination of neutralisation assays and MAAP. A recently published study of 21 patients with antineutrophil cytoplasmic antibody-associated vasculitis (AAV) showed that none of their eight rituximab-treated patients had detectable neutralising antibodies to B.1.617.2 (Delta) following the third dose of BNT162b (35). By contrast, in a small cohort of 15 AAV patients on rituximab who received a third vaccine dose, 7 (46.7%) developed measurable IgG antibodies to the S1 subunit of the SARS-CoV-2 spike protein, although the neutralisation capacity of these antibodies was not assessed (36). Humoral immune responses following the third vaccine dose among patients on anti-CD20 therapies with other autoimmune/inflammatory conditions are also impaired compared to similar patients on other immunosuppressive agents and healthy controls (14–16, 31, 46, 47). Additionally, among patients on anti-CD20 therapies who had not been seroconverted following primary vaccination, the third dose led to seroconversion rates of approximately 15%–60% (29, 32–34, 48, 49). Another small study demonstrated an inverse correlation between rituximab dose and seroconversion and showed that antibody levels persisted after a subsequent dose of rituximab among those who had already been seroconverted (50). A fall in antibody levels following a dose of

10.3389/fimmu.2023.1296148

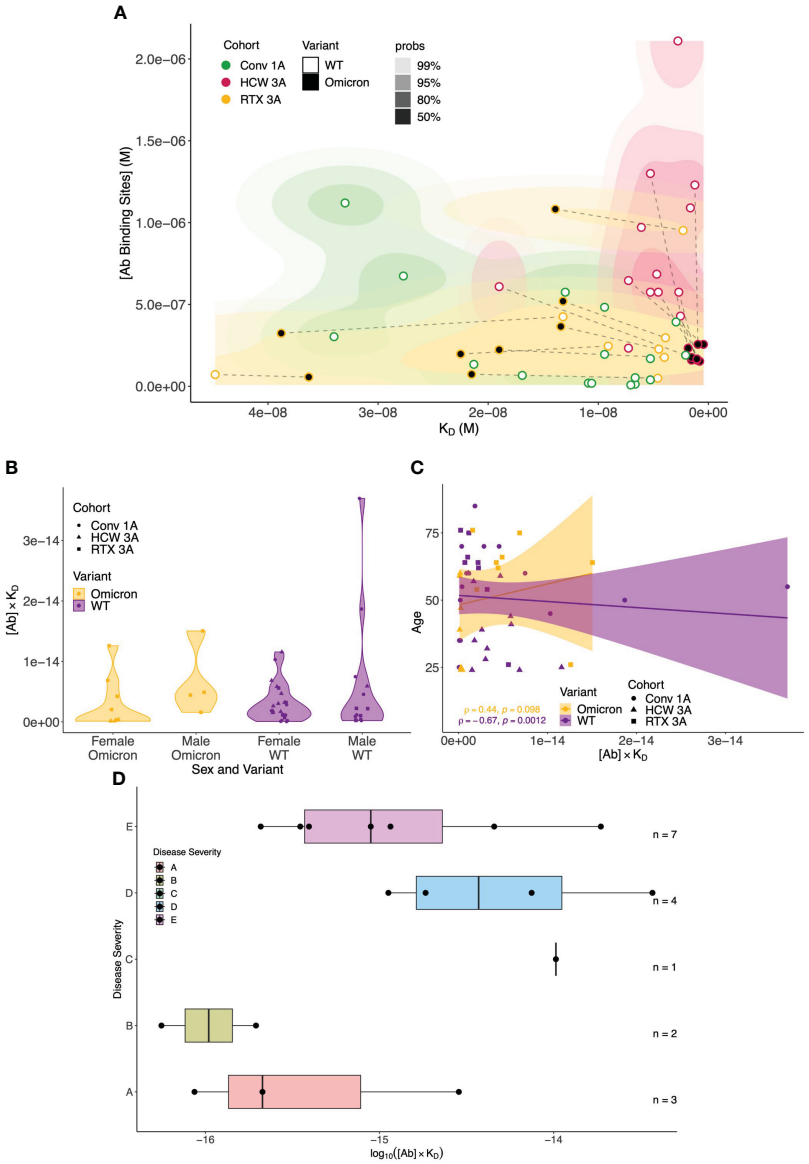

FIGURE 7
Global analysis of antibody fingerprints to SARS-CoV-2 wild-type and Omicron variants across all patient cohorts and correlation with clinically relevant parameters. **(A)** Antibody affinity and concentration across different patient cohorts and variants. The contour map summarises the equilibrium dissociation constant (K_D) *vs.* the concentration of antibody binding sites ([AB]) across three cohorts: Conv. 1A (convalescent COVID-19 at 1 month post-infection, green), RTX 3A (rituximab cohort 1 month after third vaccine dose, yellow), and HCW 3A (healthcare worker cohort 1 month after infection and two vaccinations, red); the colour gradient is proportional to the expected probability. The filling colour of points indicates the variant. Wild-type (WT) and Omicron points from the same sample are linked by dashed lines. The x-axis depicts increased affinity, i.e., lower K_D values towards the right; higher concentrations of antibody binding sites are displayed, in increasing order, on the y-axis. **(B)** Comparison of antibody affinity and concentration across sex and SARS-CoV-2 variants. The plots summarise the product of equilibrium dissociation constant (K_D) and concentration of antibody binding sites ([AB]) in relation to sex and SARS-CoV-2 variants (WT and Omicron) across three cohorts: Conv. 1A (convalescent COVID-19 at 1 month post-infection, circles), RTX 3A (rituximab cohort 1 month after third vaccine, squares), and HCW 3A (healthcare worker cohort 1 month after infection and two vaccinations, triangles). On the x-axis, the multiplicative classes on sex (male or female) and variant are represented. The y-axis represents the product of K_D and [AB] (no units). No significant differences in the product of antibody affinity and concentration were noted between female and male individuals for both Omicron ($p = 0.0617$) and WT ($p = 0.0539$); p-values are from the Mann–Whitney U test. **(C)** Comparison of antibody affinity and concentration according to patient age and SARS-CoV-2 variant. This scatter plot with a linear regression line depicts the interaction between age (y-axis) and the product of the equilibrium dissociation constant (K_D) and concentration of antibody binding sites ([AB]) (x-axis) across the variants (WT and Omicron) and cohorts: Conv. 1A (convalescent COVID-19 at 1 month post-infection, circles), RTX 3A (rituximab cohort 1 month after third vaccine, squares), and HCW 3A (healthcare worker cohort 1 month after infection and two vaccinations, triangles). A linear model fit (smooth line) and Spearman's rank correlation coefficient are depicted, indicating the strength and direction of the correlation between age and [AB] × K_D. **(D)** Relationship between COVID-19 disease severity and the product of antibody affinity and binding site concentration (log([AB] * K_D) at 1 month post-infection in the convalescent cohort. Convalescent patients after more severe disease showed a trend towards higher antibody responses ([AB] × K_D) to WT SARS-CoV-2 at 1 month after infection compared to asymptomatic patients and those with mild disease (Kruskal–Wallis rank sum test: $p = 0.08$; pairwise comparisons with Benjamini–Hochberg multiple testing correction: $p > 0.05$ for all comparisons). Disease severity was classified as follows: **(A)** asymptomatic, **(B)** mild symptoms not requiring hospitalisation, **(C)** patients who presented to hospital but never required oxygen supplementation, **(D)** patients who were admitted to hospital and whose maximal respiratory support was supplemental oxygen, and **(E)** patients who at some point required assisted ventilation.

10.3389/fimmu.2023.1296148

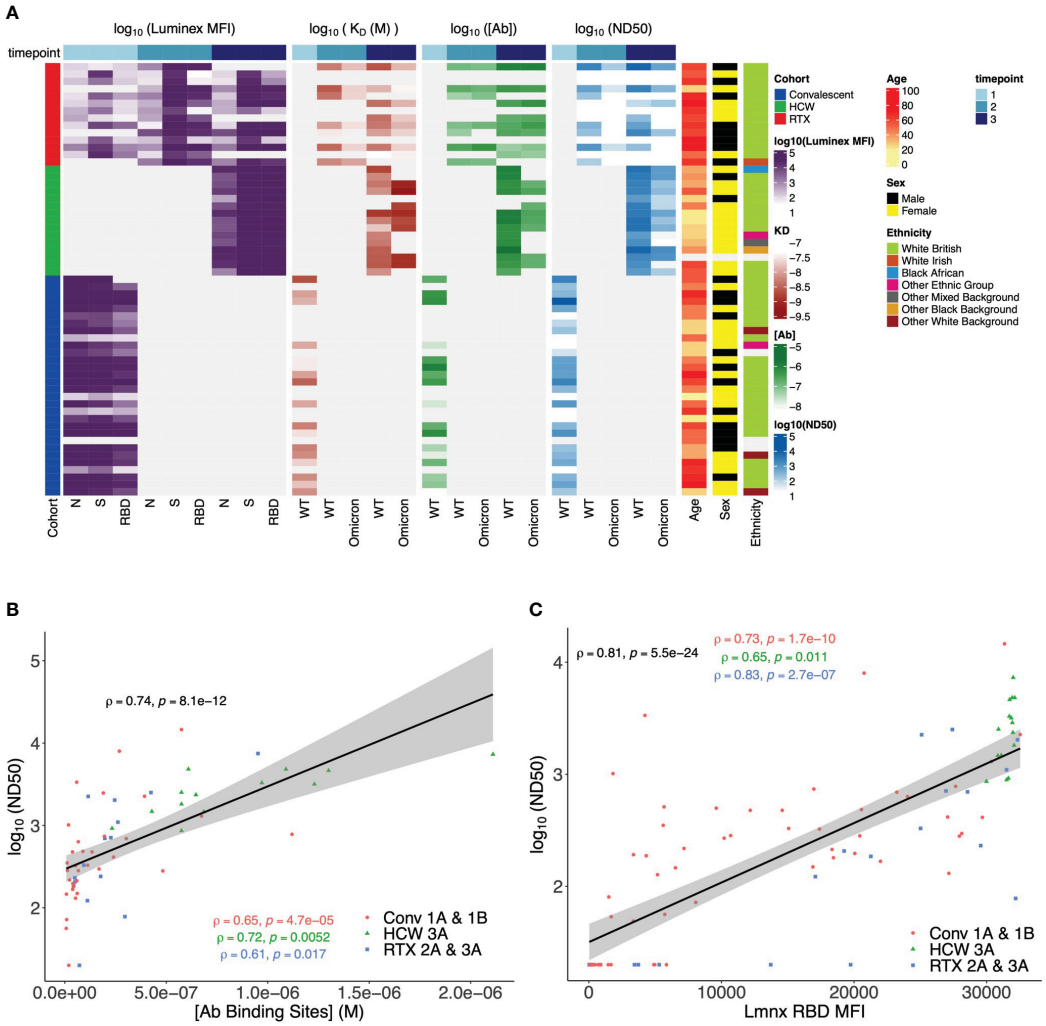

FIGURE 8
Multidimensional assessment of SARS-CoV-2 antibody profiles at the individual patient level. **(A)** Summary heatmap depicting key immunological and demographic metrics across different cohorts and timepoints. Each row corresponds to a single participant in the study, grouped per cohort affiliation (left-side colour bar). Columns correspond to several measurements, structured into four main categories: Luminex mean fluorescence intensity (MFI), K_D, [Ab], and ND_{50}. Each of these categories contains measurements at three distinct timepoints, which are denoted by the top colour bar. Luminex MFI has a breakdown into N, S, and RBD. For K_D, [Ab], and ND_{50}, measurements are differentiated by the variant of the virus (wild-type (WT) or Omicron). Colour intensity within the heatmap corresponds to the log-transformed value of each measurement, with darker hues indicating higher values (except in K_D, as lower values correspond to higher antibody affinity). Age, sex, and ethnicity of participants are also visualised in the right-side columns. **(B)** Relationship between serum wild-type SARS-CoV-2 neutralisation titre ($logND_{50}$) and antibody binding site concentration ([Ab], M) across timepoints and patient cohorts. Data points from each patient cohort are represented by different shapes. A linear model fit (smooth line) is shown, and Spearman's correlation coefficient is depicted, indicating the strength and direction of the correlation between [AB] and ND_{50}. Spearman's correlation coefficients for data in each patient cohort are also shown. **(C)** Relationship between serum wild-type SARS-CoV-2 neutralisation titre ($logND_{50}$) and Luminex anti-RBD MFI across patient cohorts. Data points from each patient cohort are represented by different colours. A linear model fit (smooth line) is shown, and Spearman's correlation coefficient is depicted, indicating the strength and direction of the correlation between ND_{50} and Luminex RBD MFI. Spearman's correlation coefficients for data in each patient cohort are also shown.

rituximab between the second and third SARS-CoV-2 vaccine doses was recently reported, although neutralisation capacity was preserved in seroconverted patients (51). In an open-label study of a fourth dose of mRNA vaccine among rituximab-treated patients, predominantly those with rheumatoid arthritis or connective tissue diseases, a moderate improvement in seroconversion from 33% to 58% was demonstrated after the fourth dose (30).

Among the patients in our cohort with detectable anti-spike antibody responses following SARS-CoV-2 vaccination, the impact of rituximab on B-cell populations, particularly memory B cells, may be of relevance to their impaired neutralising ability and affinity maturation compared to healthy controls. Memory B cells, in addition to enabling anamnestic antibody responses, also allow for the development of reactive humoral responses in the event of exposure to variant pathogens (52, 53). After vaccination, SARS-CoV-2-specific memory B cells have been shown to persist for several months, even after antibody titres have declined (54). Furthermore, the third dose of mRNA vaccine has been shown to increase the breadth and potency of memory B cells and their

antibody responses, including against Omicron (54, 55). Following rituximab treatment, memory B cells are often the last to reconstitute among peripheral blood B-cell populations (56–59), a process that can take up to several years (57). Additionally, rituximab treatment has also been associated with delays in the acquisition of somatic hypermutations among repopulated memory B cells (60). Recent data suggest that the presence of detectable peripheral circulating B cells is critical for seroconversion following vaccination among rituximab-treated patients (29), with SARS-CoV-2-specific memory B cell and plasmablast populations positively correlating with antibody titres and neutralisation (61). Furthermore, a preponderance of naïve and transitional B cells among rituximab-treated patients prior to vaccination, indicative of early B-cell reconstitution, was found to be associated with adequate humoral immune responses following vaccination (62). In support of this, improved serological responses after SARS-CoV-2 vaccination have been associated with increasing time since the last rituximab dose, particularly if this interval is more than 6 months (63, 64). Notably in our cohort, 36% of patients received rituximab within 6 months from the first vaccine dose, and 64% received an additional rituximab dose between the first and third vaccine doses, potentially accounting for the lack of improvement in the humoral response and the absence of affinity maturation between the second and third vaccine doses.

A strength of our study is that we prospectively evaluated antibody responses at specific timepoints in a relatively understudied cohort of primary systemic vasculitis patients who are particularly vulnerable to both poorer clinical outcomes from COVID-19 and impaired humoral immune responses after vaccination. Importantly, by quantifying antibody affinity and concentration directly in serum, together with data from solid-phase Luminex and neutralisation assays, we were able to provide additional insights into the quality of the immune response against WT and Omicron variants after vaccination in rituximab-treated patients. Additionally, we provide a comparative assessment with the humoral response at equivalent timepoints in non-immunocompromised cohorts after infection/vaccination and after infection only. In this regard, this is the largest study to date using a novel microfluidic assay to quantify SARS-CoV-2 antibody affinity and concentration in serum samples. The limitations of our investigations reside in the relatively small number of rituximab-treated patients included in the study and the lack of a pre-Omicron control group of previously uninfected healthy individuals with three vaccinations. Previous studies suggested differences in the abundance of IgG subclasses in anti-SARS-CoV-2 humoral responses after infection or vaccination, and it would have been interesting to quantify the relative contribution of IgG1, IgG2, IgG3, and IgG4 subclasses in our patient cohorts; however, this was not possible due to serum sample limitations (28, 65). It would have also been informative to incorporate analysis on antigen-specific T cell- and B cell-mediated cellular immunity and how this may relate to the observed serological response. Finally, the limits of sensitivity of the MAAP assay should be noted. These reflect the lower limit of labelled antigen concentration that can be employed owing to intrinsic background serum fluorescence and the fact that antibody affinity and concentration cannot be constrained in samples with low concentration and/or low-affinity antibodies (e.g., where $[Ab] < K_D$) (25).

In conclusion, our results confirm and enrich the previously reported observations of impaired humoral immune responses to SARS-CoV-2, including variants of concern, in rituximab-treated, immunosuppressed patients compared to healthy individuals. Through the addition of MAAP analysis, we highlight the significance of the fundamental parameters of the antibody response, namely, antibody affinity and concentration, to anti-viral immunity and viral escape. Consequently, should our results be replicated, we would caution against interpreting the presence of solid-phase assay-detected anti-spike antibodies following vaccination as providing evidence of immune protection against SARS-CoV-2 infection, particularly among patients on anti-CD20 therapies.

Data availability statement

The original contributions presented in the study are included in the article/Supplementary Material. Further inquiries can be directed to the corresponding author.

Ethics statement

The studies involving humans were approved by Ethics reference: 20/EM/0180 and 17/EE/0025. Please see manuscript for full details. The studies were conducted in accordance with the local legislation and institutional requirements. The participants provided their written informed consent to participate in this study.

Author contributions

AP: Data curation, Formal analysis, Writing – original draft, Writing – review & editing. MC: Writing – original draft, Writing – review & editing, Data curation. DC: Writing – review & editing, Data curation. SM: Data curation, Writing – review & editing. GM: Writing – review & editing, Formal analysis, Methodology. CX: Formal analysis, Methodology, Writing – review & editing. MH: Formal analysis, Writing – review & editing, Data curation. IG: Writing – review & editing, Methodology. RK: Writing – review & editing, Formal analysis. RD: Writing – review & editing, Data curation. JB: Writing – review & editing. IM: Writing – review & editing, Formal analysis. RJ: Writing – review & editing, Data curation, Methodology. TK: Methodology, Writing – review & editing, Conceptualization, Supervision. RS: Conceptualization, Methodology, Supervision, Writing – review & editing. VK: Writing – review & editing, Data curation, Formal analysis, Writing – original draft, Conceptualization, Supervision, Methodology.

Funding

The author(s) declare financial support was received for the research, authorship, and/or publication of this article. This study was funded in part by the University of Cambridge's Wellcome COVID-19 Rapid Response DCF (RG93172 to VK). We acknowledge funding support from the National Institute for Health Research Blood and Transplant Research Unit (NIHR BTRU, Grant number: NIHR203332) in Organ Donation and Transplantation at the University of Cambridge in collaboration with Newcastle University and in partnership with NHS Blood and Transplant (NHSBT). VK acknowledges funding from an NIHR Fellowship (PDF-2016-09-065) and as a Paul I. Terasaki Scholar (G106170). RS acknowledges funding from Addenbrooke's Charitable Trust and Vasculitis UK. RK and IM are funded by the Wellcome Trust [203151/Z/16/Z]. For the purpose of open access, the authors applied a CC BY public copyright license to all versions of the manuscript arising from this submission.

Acknowledgments

We thank all the patients and healthcare workers who consented to take part in this study. We also thank the NIHR Cambridge Biomedical Research Centre for support with sample recruitment.

Conflict of interest

TK is a member of the board of directors of Fluidic Analytics. VK provided consultancy to Fluidic Analytics Ltd (ended in 2020). Parts of this work have been the subject of a patent application filed by Cambridge Enterprise, a fully owned subsidiary of the University of Cambridge (Application Number: 17/926,780).

The remaining authors declare that the research was conducted in the absence of any commercial or financial relationships that could be construed as a potential conflict of interest.

Publisher's note

All claims expressed in this article are solely those of the authors and do not necessarily represent those of their affiliated organizations, or those of the publisher, the editors and the reviewers. Any product that may be evaluated in this article, or claim that may be made by its manufacturer, is not guaranteed or endorsed by the publisher.

Author disclaimer

The views expressed are those of the authors and not necessarily those of the National Health Service, the National Institute for Health Research, the Department of Health or National Health Service Blood and Transplant.

Supplementary material

The Supplementary Material for this article can be found online at: https://www.frontiersin.org/articles/10.3389/fimmu.2023.1296148/full#supplementary-material

References

1. Andersen KM, Bates BA, Rashidi ES, Olex AL, Mannon RB, Patel RC, et al. Long-term use of immunosuppressive medicines and in-hospital COVID-19 outcomes: a retrospective cohort study using data from the National COVID Cohort Collaborative. *Lancet Rheumatol* (2022) 4(1):e33–41. doi: 10.1016/S2665-9913(21)00325-8

2. Strangfeld A, Schafer M, GianFrancesco MA, Lawson-Tovey S, Liew JW, Ljung L, et al. Factors associated with COVID-19-related death in people with rheumatic diseases: results from the COVID-19 Global Rheumatology Alliance physician-reported registry. *Ann Rheum Dis* (2021) 80(7):930–42. doi: 10.1136/annrheumdis-2020-219498

3. Akiyama S, Hamdeh S, Micic D, Sakuraba A. Prevalence and clinical outcomes of COVID-19 in patients with autoimmune diseases: a systematic review and meta-analysis. *Ann Rheum Dis* (2021) 80(3):384–91. doi: 10.1136/annrheumdis-2020-218946

4. Agrawal U, Bedston S, McCowan C, Oke J, Patterson L, Robertson C, et al. Severe COVID-19 outcomes after full vaccination of primary schedule and initial boosters: pooled analysis of national prospective cohort studies of 30 million individuals in England, Northern Ireland, Scotland, and Wales. *Lancet* (2022) 400(10360):1305–20. doi: 10.1016/S0140-6736(22)01656-7

5. Schietzel S, Anderegg M, Limacher A, Born A, Horn MP, Maurer B, et al. Humoral and cellular immune responses on SARS-CoV-2 vaccines in patients with anti-CD20 therapies: a systematic review and meta-analysis of 1342 patients. *RMD Open* (2022) 8(1):e002036. doi: 10.1136/rmdopen-2021-002036

6. Galmiche S, Luong Nguyen LB, Tartour E, de Lamballerie X, Wittkop L, Loubet P, et al. Immunological and clinical efficacy of COVID-19 vaccines in immunocompromised populations: a systematic review. *Clin Microbiol Infect* (2022) 28(2):163–77. doi: 10.1016/j.cmi.2021.09.036

7. Ferri C, Ursini F, Gragnani L, Raimondo V, Giuggioli D, Foti R, et al. Impaired immunogenicity to COVID-19 vaccines in autoimmune systemic diseases. High prevalence of non-response in different patients' subgroups. *J Autoimmun* (2021) 125:102744. doi: 10.1016/j.jaut.2021.102744

8. UK Health Secruity Agency. *COVID-19: the green book, chapter 14a The Green Book*. (2022).

9. World Health Organization. *Good practice statement on the use of second booster doses for COVID-19 vaccines*. (2022).

10. Centres for Disease Control and Prevention (CDC). *COVID-19 Vaccines for People Who Are Moderately or Severely Immunocompromised* (2022). Available at: https://www.cdc.gov/coronavirus/2019-ncov/vaccines/recommendations/immuno.html.

11. Stevens KI, Frangou E, Shin JIL, Anders HJ, Bruchfeld A, Schonermarck U, et al. Perspective on COVID-19 vaccination in patients with immune-mediated kidney diseases: consensus statements from the ERA-IWG and EUVAS. *Nephrol Dial Transpl* (2022) 37(8):1400–10. doi: 10.1093/ndt/gfac052

12. Lee A, Wong SY, Chai LYA, Lee SC, Lee MX, Muthiah MD, et al. Efficacy of covid-19 vaccines in immunocompromised patients: systematic review and meta-analysis. *BMJ* (2022) 376:e068632. doi: 10.1136/bmj-2021-068632

13. Vijenthira A, Gong I, Betschel SD, Cheung M, Hicks LK. Vaccine response following anti-CD20 therapy: a systematic review and meta-analysis of 905 patients. *Blood Adv* (2021) 5(12):2624–43. doi: 10.1182/bloodadvances.2021004629

14. Wieske L, van Dam KPJ, Steenhuis M, Stalman EW, Kummer LYL, van Kempen ZLE, et al. Humoral responses after second and third SARS-CoV-2 vaccination in patients with immune-mediated inflammatory disorders on immunosuppressants: a

cohort study. *Lancet Rheumatol* (2022) 4(5):e338–e50. doi: 10.1016/S2665-9913(22)00034-0

15. Jyssum I, Kared H, Tran TT, Tveter AT, Provan SA, Sexton J, et al. Humoral and cellular immune responses to two and three doses of SARS-CoV-2 vaccines in rituximab-treated patients with rheumatoid arthritis: a prospective, cohort study. *Lancet Rheumatol* (2022) 4(3):e177–e87. doi: 10.1016/S2665-9913(21)00394-5

16. Firinu D, Fenu G, Sanna G, Costanzo GA, Perra A, Campagna M, et al. Evaluation of humoral and cellular response to third dose of BNT162b2 mRNA COVID-19 vaccine in patients treated with B-cell depleting therapy. *J Autoimmun* (2022) 131:102848. doi: 10.1016/j.jaut.2022.102848

17. Cromer D, Steain M, Reynaldi A, Schlub TE, Wheatley AK, Juno JA, et al. Neutralising antibody titres as predictors of protection against SARS-CoV-2 variants and the impact of boosting: a meta-analysis. *Lancet Microbe* (2022) 3(1):e52–61. doi: 10.1016/S2666-5247(21)00267-6

18. Cheng SMS, Mok CKP, Leung YWY, Ng SS, Chan KCK, Ko FW, et al. Neutralizing antibodies against the SARS-CoV-2 Omicron variant BA.1 following homologous and heterologous CoronaVac or BNT162b2 vaccination. *Nat Med* (2022) 28(3):486–9. doi: 10.1038/s41591-022-01704-7

19. Bowen JE, Addetia A, Dang HV, Stewart C, Brown JT, Sharkey WK, et al. Omicron spike function and neutralizing activity elicited by a comprehensive panel of vaccines. *Science* (2022) 377(6608):890–4. doi: 10.1126/science.abq0203

20. Hachmann NP, Miller J, Collier AY, Ventura JD, Yu J, Rowe M, et al. Neutralization escape by SARS-CoV-2 omicron subvariants BA.2.12.1, BA.4, and BA.5. *N Engl J Med* (2022) 387(1):86–8. doi: 10.1056/NEJMc2212117

21. Willett BJ, Grove J, MacLean OA, Wilkie C, De Lorenzo G, Furnon W, et al. SARS-CoV-2 Omicron is an immune escape variant with an altered cell entry pathway. *Nat Microbiol* (2022) 7(8):1161–79. doi: 10.1038/s41564-022-01143-7

22. McCallum M, Walls AC, Sprouse KR, Bowen JE, Rosen LE, Dang HV, et al. Molecular basis of immune evasion by the Delta and Kappa SARS-CoV-2 variants. *Science* (2021) 374(6575):1621–6. doi: 10.1126/science.abl8506

23. Kent SJ, Khoury DS, Reynaldi A, Juno JA, Wheatley AK, Stadler E, et al. Disentangling the relative importance of T cell responses in COVID-19: leading actors or supporting cast? *Nat Rev Immunol* (2022) 22(6):387–97. doi: 10.1038/s41577-022-00716-1

24. Wherry EJ, Barouch DH. T cell immunity to COVID-19 vaccines. *Science* (2022) 377(6608):821–2. doi: 10.1126/science.add2897

25. Schneider MM, Scheidt T, Priddey AJ, Xu CK, Hu M, Meisl G, et al. Microfluidic antibody affinity profiling of alloantibody-HLA interactions in human serum. *Biosens Bioelectron* (2023) 228:115196. doi: 10.1016/j.bios.2023.115196

26. Schneider MM, Emmenegger M, Xu CK, Condado Morales I, Meisl G, Turelli P, et al. Microfluidic characterisation reveals broad range of SARS-CoV-2 antibody affinity in human plasma. *Life Sci Alliance* (2021) 5(2):e202101270. doi: 10.26508/lsa.202101270

27. Denninger V, Xu CK, Meisl G, Morgunov AS, Fiedler S, Ilsley A, et al. Microfluidic antibody affinity profiling reveals the role of memory reactivation and cross-reactivity in the defense against SARS-CoV-2. *ACS Infect Dis* (2022) 8(4):790–9. doi: 10.1021/acsinfecdis.1c00486

28. Emmenegger M, Fiedler S, Brugger SD, Devenish SRA, Morgunov AS, Ilsley A, et al. Both COVID-19 infection and vaccination induce high-affinity cross-clade responses to SARS-CoV-2 variants. *iScience* (2022) 25(8):104766. doi: 10.1016/j.isci.2022.104766

29. Ammitzboll C, Kragh Thomsen M, Bogh Andersen J, Jensen JMB, From Hermansen ML, Dahl Johannsen A, et al. Rituximab-treated rheumatic patients: B-cells predict seroconversion after COVID-19 boost or revaccination in initial vaccine non-responders. *Rheumatol (Oxford)* (2023) 62(7):2544–9. doi: 10.1093/rheumatology/keac666

30. Mrak D, Simader E, Sieghart D, Mandl P, Radner H, Perkmann T, et al. Immunogenicity and safety of a fourth COVID-19 vaccination in rituximab-treated patients: an open-label extension study. *Ann Rheum Dis* (2022) 81:1750–6. doi: 10.1136/ard-2022-222579

31. Sidler D, Born A, Schietzel S, Horn MP, Aeberli D, Amsler J, et al. Trajectories of humoral and cellular immunity and responses to a third dose of mRNA vaccines against SARS-CoV-2 in patients with a history of anti-CD20 therapy. *RMD Open* (2022) 8(1). doi: 10.1136/rmdopen-2021-002166

32. Bitoun S, Avouac J, Henry J, Ghossan R, Al Tabaa O, Belkhir R, et al. Very low rate of humoral response after a third COVID-19 vaccine dose in patients with autoimmune diseases treated with rituximab and non-responders to two doses. *RMD Open* (2022) 8(1). doi: 10.1136/rmdopen-2022-002308

33. Bonelli M, Mrak D, Tobudic S, Sieghart D, Koblischke M, Mandl P, et al. Additional heterologous versus homologous booster vaccination in immunosuppressed patients without SARS-CoV-2 antibody seroconversion after primary mRNA vaccination: a randomised controlled trial. *Ann Rheum Dis* (2022) 81(5):687–94. doi: 10.1136/annrheumdis-2021-221558

34. Simon D, Tascilar K, Fagni F, Schmidt K, Kronke G, Kleyer A, et al. Efficacy and safety of SARS-CoV-2 revaccination in non-responders with immune-mediated inflammatory disease. *Ann Rheum Dis* (2022) 81(7):1023–7. doi: 10.1136/annrheumdis-2021-221554

35. Speer C, Tollner M, Benning L, Klein K, Bartenschlager M, Nusshag C, et al. Third COVID-19 vaccine dose with BNT162b2 in patients with ANCA-associated vasculitis. *Ann Rheum Dis* (2022) 81(4):593–5. doi: 10.1136/annrheumdis-2021-221747

36. Kant S, Azar A, Geetha D. Antibody response to COVID-19 booster vaccine in rituximab-treated patients with anti-neutrophil cytoplasmic antibody-associated vasculitis. *Kidney Int* (2022) 101(2):414–5. doi: 10.1016/j.kint.2021.11.012

37. Marty PK, Van Keulen VP, Erskine CL, Shah M, Hummel A, Stachowitz M, et al. Antigen specific humoral and cellular immunity following SARS-CoV-2 vaccination in ANCA-associated vasculitis patients receiving B-cell depleting therapy. *Front Immunol* (2022) 13:834981. doi: 10.3389/fimmu.2022.834981

38. Smith RM, Cooper DJ, Doffinger R, Stacey H, Al-Mohammad A, Goodfellow I, et al. SARS-COV-2 vaccine responses in renal patient populations. *BMC Nephrol* (2022) 23(1):199. doi: 10.1186/s12882-022-02792-w

39. Cooper DJ, Lear S, Watson L, Shaw A, Ferris M, Doffinger R, et al. A prospective study of risk factors associated with seroprevalence of SARS-CoV-2 antibodies in healthcare workers at a large UK teaching hospital. *J Infect* (2022) 85(5):557–64. doi: 10.1016/j.jinf.2022.08.030

40. Bergamaschi L, Mescia F, Turner L, Hanson AL, Kotagiri P, Dunmore BJ, et al. Longitudinal analysis reveals that delayed bystander CD8+ T cell activation and early immune pathology distinguish severe COVID-19 from mild disease. *Immunity* (2021) 54(6):1257–75.e8. doi: 10.1016/j.immuni.2021.05.010

41. Xiong X, Qu K, Ciazynska KA, Hosmillo M, Carter AP, Ebrahimi S, et al. A thermostable, closed SARS-CoV-2 spike protein trimer. *Nat Struct Mol Biol* (2020) 27(10):934–41. doi: 10.1038/s41594-020-0478-5

42. Collier DA, De Marco A, Ferreira IATM, Meng B, Datir RP, Walls AC, et al. Sensitivity of SARS-CoV-2 B.1.1.7 to mRNA vaccine-elicited antibodies. *Nature* (2021) 593(7857):136–41. doi: 10.1038/s41586-021-03412-7

43. Bellusci L, Grubbs G, Zahra FT, Forgacs D, Golding H, Ross TM, et al. Antibody affinity and cross-variant neutralization of SARS-CoV-2 Omicron BA.1, BA.2 and BA.3 following third mRNA vaccination. *Nat Commun* (2022) 13(1):4617. doi: 10.1038/s41467-022-32298-w

44. Cho A, Muecksch F, Schaefer-Babajew D, Wang Z, Finkin S, Gaebler C, et al. Anti-SARS-CoV-2 receptor-binding domain antibody evolution after mRNA vaccination. *Nature* (2021) 600(7889):517–22. doi: 10.1038/s41586-021-04060-7

45. Kim W, Zhou JQ, Horvath SC, Schmitz AJ, Sturtz AJ, Lei T, et al. Germinal centre-driven maturation of B cell response to mRNA vaccination. *Nature* (2022) 604(7904):141–5. doi: 10.1038/s41586-022-04527-1

46. Aikawa NE, Kupa LVK, Medeiros-Ribeiro AC, Saad CGS, Yuki EFN, Pasoto SG, et al. Increment of immunogenicity after third dose of a homologous inactivated SARS-CoV-2 vaccine in a large population of patients with autoimmune rheumatic diseases. *Ann Rheum Dis* (2022) 81(7):1036–43. doi: 10.1136/annrheumdis-2021-222096

47. Bajwa HM, Novak F, Nilsson AC, Nielsen C, Holm DK, Ostergaard K, et al. Persistently reduced humoral and sustained cellular immune response from first to third SARS-CoV-2 mRNA vaccination in anti-CD20-treated multiple sclerosis patients. *Mult Scler Relat Disord* (2022) 60:103729. doi: 10.1016/j.msard.2022.103729

48. Herishanu Y, Rahav G, Levi S, Braester A, Itchaki G, Bairey O, et al. Efficacy of a third BNT162b2 mRNA COVID-19 vaccine dose in patients with CLL who failed standard 2-dose vaccination. *Blood* (2022) 139(5):678–85. doi: 10.1182/blood.2021014085

49. Funakoshi Y, Yakushijin K, Ohji G, Hojo W, Sakai H, Watanabe M, et al. Promising efficacy of a third dose of mRNA SARS-CoV-2 vaccination in patients treated with anti-CD20 antibody who failed 2-dose vaccination. *Vaccines (Basel)* (2022) 10(6):965. doi: 10.3390/vaccines10060965

50. van der Togt CJT, Ten Cate DF, van den Bemt BJF, Rahamat-Langendoen J, den Broeder N, den Broeder AA. Seroconversion after a third COVID-19 vaccine is affected by rituximab dose but persistence is not in patients with rheumatoid arthritis. *Rheumatol (Oxford)* (2023) 62(4):1627–30. doi: 10.1093/rheumatology/keac486

51. Stefanski AL, Rincon-Arevalo H, Schrezenmeier E, Karberg K, Szelinski F, Ritter J, et al. Persistent but atypical germinal center reaction among 3(rd) SARS-CoV-2 vaccination after rituximab exposure. *Front Immunol* (2022) 13:943476. doi: 10.3389/fimmu.2022.943476

52. Akkaya M, Kwak K, Pierce SK. B cell memory: building two walls of protection against pathogens. *Nat Rev Immunol* (2020) 20(4):229–38. doi: 10.1038/s41577-019-0244-2

53. Purtha WE, Tedder TF, Johnson S, Bhattacharya D, Diamond MS. Memory B cells, but not long-lived plasma cells, possess antigen specificities for viral escape mutants. *J Exp Med* (2011) 208(13):2599–606. doi: 10.1084/jem.20110740

54. Goel RR, Painter MM, Lundgreen KA, Apostolidis SA, Baxter AE, Giles JR, et al. Efficient recall of Omicron-reactive B cell memory after a third dose of SARS-CoV-2 mRNA vaccine. *Cell* (2022) 185(11):1875–87 e8. doi: 10.1016/j.cell.2022.04.009

55. Muecksch F, Wang Z, Cho A, Gaebler C, Ben Tanfous T, DaSilva J, et al. Increased memory B cell potency and breadth after a SARS-CoV-2 mRNA boost. *Nature* (2022) 607(7917):128–34. doi: 10.1038/s41586-022-04778-y

56. Leandro MJ, Cambridge G, Ehrenstein MR, Edwards JC. Reconstitution of peripheral blood B cells after depletion with rituximab in patients with rheumatoid arthritis. *Arthritis Rheumatol* (2006) 54(2):613–20. doi: 10.1002/art.21617

57. Anolik JH, Barnard J, Owen T, Zheng B, Kemshetti S, Looney RJ, et al. Delayed memory B cell recovery in peripheral blood and lymphoid tissue in systemic lupus erythematosus after B cell depletion therapy. *Arthritis Rheumatol* (2007) 56(9):3044–56. doi: 10.1002/art.22810

58. Colucci M, Carsetti R, Cascioli S, Casiraghi F, Perna A, Rava L, et al. B cell reconstitution after rituximab treatment in idiopathic nephrotic syndrome. *J Am Soc Nephrol* (2016) 27(6):1811–22. doi: 10.1681/ASN.2015050523

59. Roll P, Dorner T, Tony HP. Anti-CD20 therapy in patients with rheumatoid arthritis: predictors of response and B cell subset regeneration after repeated treatment. *Arthritis Rheumatol* (2008) 58(6):1566–75. doi: 10.1002/art.23473

60. Muhammad K, Roll P, Einsele H, Dorner T, Tony HP. Delayed acquisition of somatic hypermutations in repopulated IGD+CD27+ memory B cell receptors after rituximab treatment. *Arthritis Rheumatol* (2009) 60(8):2284–93. doi: 10.1002/art.24722

61. Stefanski AL, Rincon-Arevalo H, Schrezenmeier E, Karberg K, Szelinski F, Ritter J, et al. B cell numbers predict humoral and cellular response upon SARS-CoV-2 vaccination among patients treated with rituximab. *Arthritis Rheumatol* (2022) 74 (6):934–47. doi: 10.1002/art.42060

62. Stefanski AL, Rincon-Arevalo H, Schrezenmeier E, Karberg K, Szelinski F, Ritter J, et al. B cell characteristics at baseline predict vaccination response in RTX treated patients. *Front Immunol* (2022) 13:822885. doi: 10.3389/fimmu.2022.822885

63. Bitoun S, Henry J, Desjardins D, Vauloup-Fellous C, Dib N, Belkhir R, et al. Rituximab impairs B cell response but not T cell response to COVID-19 vaccine in autoimmune diseases. *Arthritis Rheumatol* (2022) 74(6):927–33. doi: 10.1002/art.42058

64. Jinich S, Schultz K, Jannat-Khah D, Spiera R. B cell reconstitution is strongly associated with COVID-19 vaccine responsiveness in rheumatic disease patients who received treatment with rituximab. *Arthritis Rheumatol* (2022) 74(5):776–82. doi: 10.1002/art.42034

65. Amanat F, Stadlbauer D, Strohmeier S, Nguyen THO, Chromikova V, McMahon M, et al. A serological assay to detect SARS-CoV-2 seroconversion in humans. *Nat Med* (2020) 26(7):1033–6. doi: 10.1038/s41591-020-0913-5